International Journal of Environmental Sciences
ISSN: 2229-7359
Vol. 11 No. 21s, 2025
https://theaspd.com/index.php

Improvised Fuzzy Logic Controller Using Feedforward, Feedback Offset, And Proportional Integral For Knee Extension Rehabilitation With Nonlinearities Influences

S. Arof[1,2], E. Noorsal[1], S.Z. Yahaya[1], Z. Hussain[1], M.K. Safie[1,3], Y.M. Ali[1], M.H. Abdullah[1], S. Setumin[1]
[1]Electrical Engineering Studies, Universiti Teknologi MARA Cawangan Pulau Pinang, Permatang Pauh Campus,13500, Pulau Pinang, Malaysia.
[2]Universiti Kuala Lumpur, Malaysian Spanish Institute Kulim Hi-Tech Park, 09000 Kulim, Kedah, Malaysia.
[3]Intel PG14, Plot 6, Medan Bayan Lepas, Bayan Lepas Technoplex, Bayan Lepas 11900, Pulau Pinang, Malaysia.
Corresponding Author*: emilia.noorsal@uitm.edu.my

ABSTRACT:
Rehabilitation through exercise using functional electrical stimulation (FES) is an effective approach to aiding recovery for individuals with spinal cord injuries (SCI). FES devices induce muscle contractions via electrode pads, generating force and torque. Precise control is essential to prevent overstimulation, which could lead to fatigue, pain, or injury. However, nonlinear effects such as fatigue, spasticity, and time delays pose challenges to feedback control systems, often resulting in performance degradation. Fuzzy logic controllers (FLCs) are known for their robustness in addressing these issues but face constraints in control bandwidth and time delay management, which can lead to oscillations. This study proposes an enhanced FLC by designing fuzzy input membership functions, rules, and outputs and incorporating tuning strategies to address these limitations. Additionally, the integration of feedback offset, and proportional-integral strategies is emphasized to improve control bandwidth and mitigate the effects of time delays. The proposed control algorithm is simulated and evaluated using MATLAB/Simulink in the context of knee extension rehabilitation, which is characterized by nonlinearities. The results demonstrated that the newly enhanced FLC architecture could effectively overcome bandwidth and time delay challenges, validating its suitability for knee extension rehabilitation in SCI patients.

KEYWORDS**: **Rehabilitation, FES, Veltink Model, Knee Extension, Non-linearities, Time Delay, Fuzzy Logic Controller

1 INTRODUCTION

Functional electrical stimulation (FES) devices are widely utilized for restoring movement function in paralyzed muscles and limbs. A significant challenge in FES applications is the effect of nonlinearities, which can lead to premature muscle fatigue in users undergoing treatment [1]. Closed-loop control algorithms are designed to enhance the performance of open-loop systems [2]. However, in FES applications, the effectiveness of closed-loop controllers tends to deteriorate under nonlinear conditions such as fatigue [3], stiffness, time delay, and spasticity [4-7]. Additionally, accurately identifying a model in clinical settings is often impractical due to time constraints and changing dynamics [8, 9], making tuning of closed-loop controllers feasible only during simulation stages.

Various feedback controllers have been implemented for controlling knee extension rehabilitation, including conventional PID [10], Sliding Mode [11], Fuzzy Logic [12, 13], Neural Networks [13], and Adaptive Controllers [14]. Comparative studies of closed-loop controller performance in knee extension applications indicate that while PID controllers are simple and easy to implement, their performance is relatively low. In contrast, Neural Networks (NN) offer superior performance. Still, they are complicated to implement in hardware, lack a mathematical model, and suffer from stability issues, slow online adaptation, and the need for offline training [15]. Sliding Mode controllers are known for their robustness and fast tuning but face challenges such as chattering and the need for a mathematical model to design the sliding surface. Adaptive controllers are complex, costly, and time-consuming to set up and tune. The FLC is considered user-friendly for real-world implementation, can be tuned online, do not require a mathematical model, exhibits less chattering, and outperforms PID controllers [16]. However, the FLC faces bandwidth issues, limiting its effectiveness at certain reference points [12, 17], and can lead to oscillations in the presence of time delays [12].

International Journal of Environmental Sciences
ISSN: 2229-7359
Vol. 11 No. 21s, 2025
https://theaspd.com/index.php

The primary objective of this research is to develop and refine a closed-loop FLC for rehabilitation through knee extension exercises using FES, addressing both the presence and absence of nonlinear effects (fatigue, stiffness, spasticity and time delay). The Veltink model of knee extension, with and without nonlinearities, is the basis for simulating patient conditions during rehabilitation exercises. This study thoroughly details the setup and ongoing improvements of the FLC, representing an initial phase in preparing the controller for adaptation into a system capable of managing rehabilitation under the influence of nonlinearities.

2 METHODS

This section outlines the design methodology, beginning with developing the knee extension model and integrating nonlinearities. The process includes the development of the FLC, gain tuning, and enhancements using feedforward offsetting and a proportional-integral (PI) FLC to address discrepancies when managing linear and nonlinear conditions. The design process culminates in a comprehensive system simulation, incorporating the knee model and the FLC within the MATLAB/Simulink environment. Additionally, the methodology introduces concepts such as using offsets and accumulators in the FLC. After determining all gain parameters, the FLC and knee model were developed and tested in MATLAB/Simulink to evaluate their performance.

2.1 Knee Extension Model

Electrically stimulated charges applied to muscles are modelled within biomechanics and utilized in a controlled study of ankle joint movement. The knee extension model, which requires specific system parameters and dynamics, is developed using the method established by Veltink et al [12, 18]. Veltink employed equations to define the relationship between torque and angular movement. The mathematical framework for describing these dynamics consists of linear differential equations and transfer functions. These equations form the foundation for the physically based knee extension model, facilitating an understanding the intricate interplay between electrical stimulation, muscle response, and joint movement, which is essential for tuning the FLC.

To further evaluate the capabilities of the FLC, a simulation model was developed that incorporates nonlinear effects, including fatigue, spasticity, stiffness, and time delay. These factors significantly impact muscle torque and the knee trajectory response. The block module representing the system with these nonlinearities is illustrated in Figure 1 . The simplified mathematical expressions for damping, stiffness, spasticity, and FES pulse width charges are provided in Equation (1) [5]. The effects of fatigue and time delay are also discussed in references [5, 12, 18].

$$\begin{aligned} \therefore \sum: \dot{x}(t) = \frac{1}{J}\Big(-mgl(t) - \lambda e^{-E\left(x_1+\frac{\pi}{2}\right)} \\ + \left(x_1(t) + \frac{\pi}{2} - w\right) - Tspasm(t)\bar{l}sin\,\pi - \phi(t) \\ -(\pi/2 - \theta(t)) - Bx_2 + \frac{G}{\eta}e^{\frac{-t}{\eta}} * u(t)\mu(t) \end{aligned} \quad (1)$$

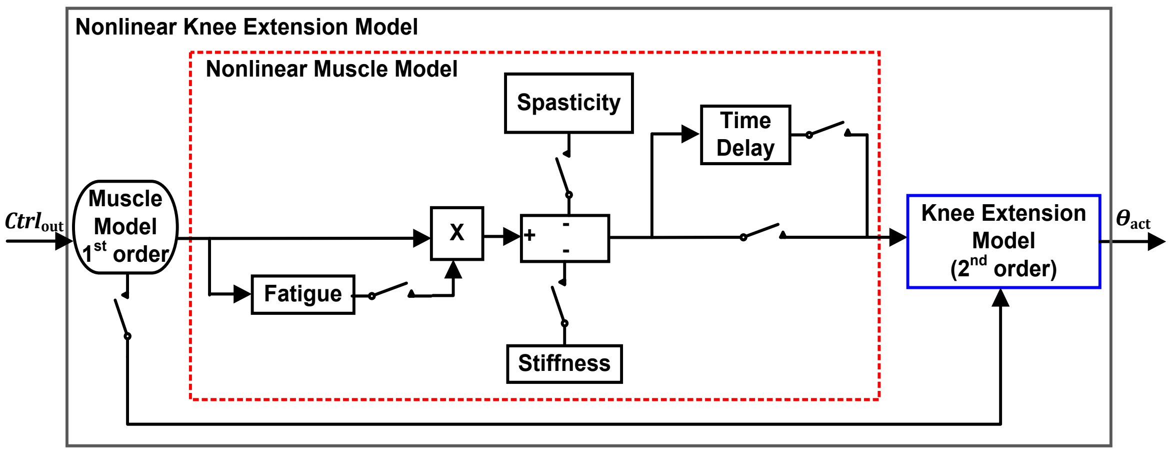

Figure 1 The internal architecture of the knee extension model with nonlinearities [13].

2.2 Closed Loop Feedback Control using Fuzzy Logic

The system overview of a typical closed-loop FES-assisted knee extension exercise in a closed-loop system mainly consists of a non-linear knee extension model and FLC, as illustrated in Figure 2.

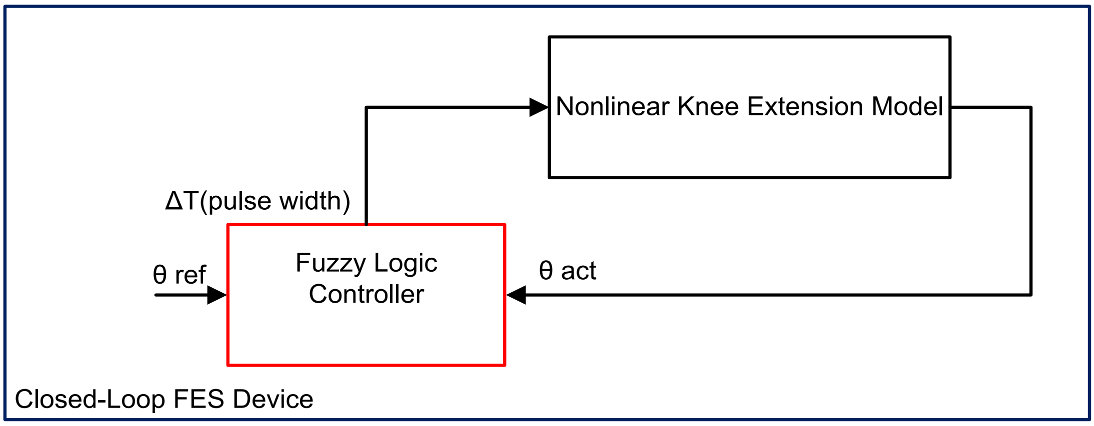

Figure 2 System overview of closed-loop functional electrical stimulation (FES).

The FLC architecture is shown in Figure 3. The FLC mainly consists of fuzzification, rules, inference and defuzzification. The knee extension's target or maximum reference angle (Θ_{ref}) is set as the FLC input. From the reference angle (Θ_{ref}) and the actual knee angular position (Θ_{act}), the error and rate of error are generated. Based on the selected error and rate of error, the FLC provides the required output amount for the pulse width duration.

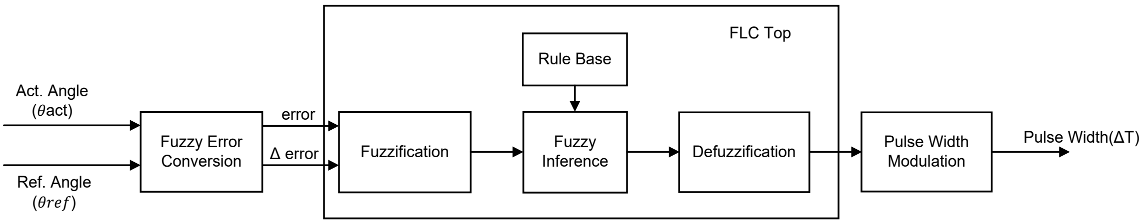

Figure 3 Fuzzy logic overview architecture.

Fuzzification, Rule Base, Fuzzy Inference and Defuzzification of the FLC are interrelated to the fuzzy logic membership functions of input variables, singleton fuzzy output, and fuzzy rules. The membership functions shown in Figure 4 are the input for error and fuzzy logic rate of error. The distance between s1, s2 and s3 is changeable depending on the overall fuzzy logic performance.

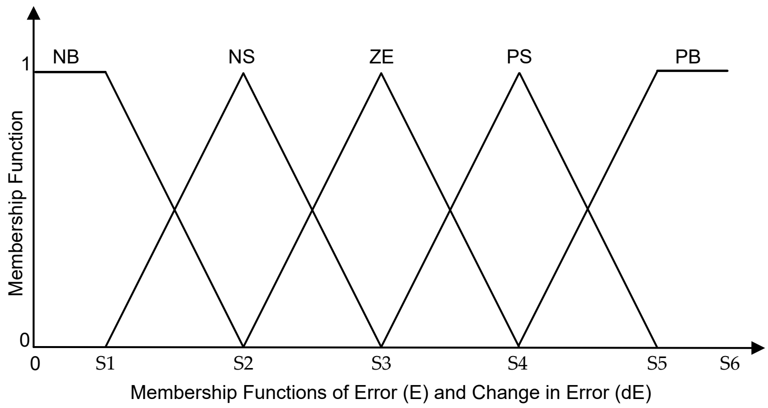

Figure 4 Fuzzy Logic membership function

The singleton fuzzy logic output is shown in Figure 5. The value of the singleton is changeable depending on the overall fuzzy logic performance.

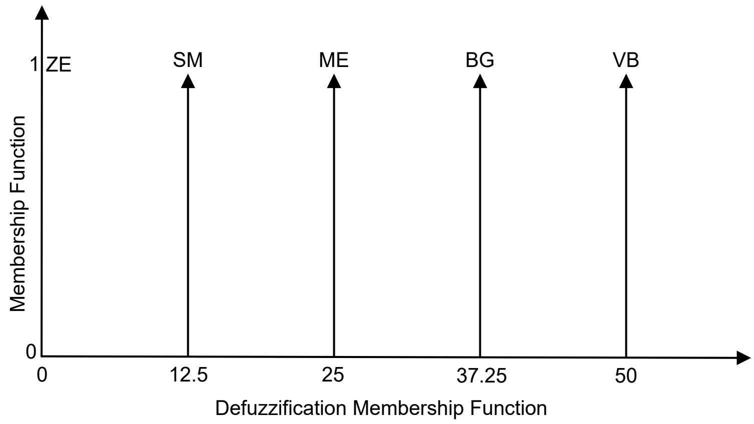

Figure 5 Fuzzy logic output singleton.

An example of fuzzy logic rules is shown in Table 1. The table rules influence overall fuzzy logic performance.

Table 1 Fuzzy rule base table for knee extension.

		Input1 - Error (E)				
		NB	NS	ZE	PS	PB
Input 2 - Change in Error (dE)	NB	VS (min1)	VS (min2)	VS (min3)	SM (min4)	ME (min5)
	NS	VS (min6)	VS (min7)	SM (min8)	ME (min9)	BG (min10)
	ZE	VS (min11)	SM (min12)	ME (min13)	BG (min14)	VB (min15)
	PS	SM (min16)	ME (min17)	BG (min18)	VB (min19)	VB (min20)
	PB	ME (min21)	BG (min22)	VB (min23)	VB (min24)	VB (min25)

2.2.1 Initial Close Loop Fuzzy Logic System Tuning using Trial and Error Settings

The methodology for tuning the FLC involves adjusting the membership functions of the input variables, the singleton fuzzy output, and the fuzzy rules. Firstly, the membership functions for the input variables, such as error and rate of error, can be modified to better represent the system's operating conditions [19, 20]. By fine-tuning the shapes, widths, and positions of these membership functions, the controller can adapt to changes in the system dynamics and provide more accurate control responses. Secondly, the singleton fuzzy output can be adjusted to fine-tune the control actions [21]. The singleton values determine the crisp output of the fuzzy logic system, and by optimizing these values, the controller can enhance its ability to compensate for the time delay effects and improve the closed-loop control bandwidth. Finally, the fuzzy rules governing the input-output mapping can be refined to better capture the logical relationships between the system variables. Adjusting the fuzzy rules allows the controller to make more informed decisions and provide more effective control actions, further contributing to the improvement of the closed-loop control bandwidth and mitigation of time delay issues. Through this iterative process of tuning the membership functions, output, and fuzzy rules, the FLC can be optimized to achieve the desired performance in terms of enhancing the closed-loop control bandwidth and addressing the challenges posed by time delay systems.

This study selected the Sugeno FLC for the closed-loop control response due to its simplicity and linearity [12, 19]. In a feedback closed-loop system, the primary focus is on how the control changes in response to variations in error and rate of error. The initial tuning process involves conducting an open-loop test to identify the error and rate of error patterns, which are essential for preparing the membership functions. Examples of these patterns are illustrated in Figure 6 and Figure 7 below.

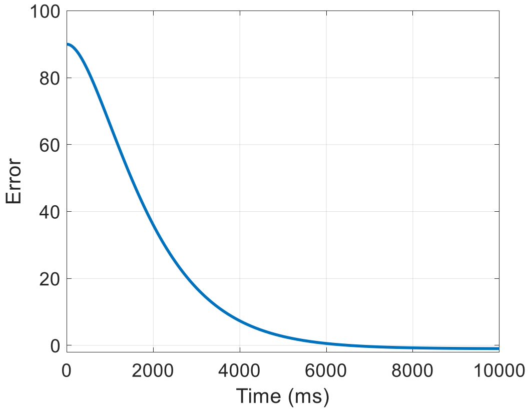

Figure 6 Open loop Error

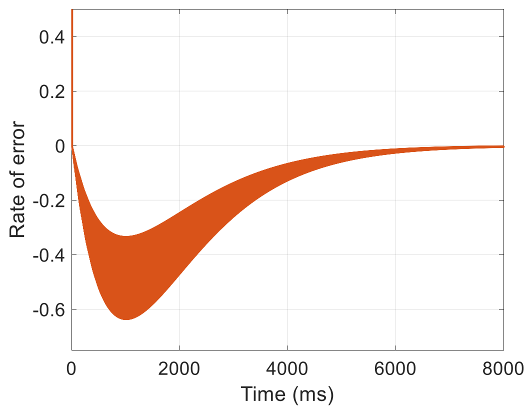

Figure 7 Error rate of the open loop response

The analysis of the open-loop test concerning error and rate-of-error reveals that the maximum rate-of-error fluctuates between 0.36 and 0.63. The steady-state time required to reach the final output angle is 8 seconds. While there is a 2° overshoot, no oscillation is observed during the process. Additionally, achieving 50% of the final output angle is 2 seconds, with a final steady-state error of 2°. These results provide valuable insights into the performance characteristics of the FLC.

In the initial setup of the closed-loop fuzzy logic trial and error settings, the fuzzy input membership functions (MF) for error and rate-of-error are presented in Table 2. Both sets of membership functions are triangular shapes, with a single Sugeno output corresponding to one final output signal. The error membership functions include 'negative medium' (NM), 'negative small' (NS), 'zero' (Z), 'positive small' (PS), and 'positive big' (PB). The boundaries for these error membership functions are equally divided, and the maximum value is set to be less than one-fifth of the maximum input value, as indicated in Table 2. This configuration establishes a foundational framework for the FLC's performance.

The membership functions for the rate of error include 'negative big' (NB), 'negative small' (NS), 'zero' (Z), 'positive small' (S), and 'positive big' (B). As indicated in Table 2, the boundaries of these membership functions are not equally divided; the negative side is significantly larger than the positive side. This configuration is established based on the results from the open-loop test, reflecting the dynamics of the system being controlled.

Table 2 Membership Function (MF) of Error (E) and Rate of Error (dE). The input MFs are Negative Medium (NM), Negative Small (NS), Zero (Z), Positive Small (S) and Positive Big (PB).

MF	Error (E)	Rate of Error (dE)
NM	-10, -10, -5	-0.22, -0.22, -0.11
NS	-10, - 5, 0	-0.22, -0.11, 0
Z	-5, 0, 5	-0.025, 0, 0.025
PS	0, 5,10	0, 0.11, 0.22
PB	5, 10, 10	0.11, 0.22, 0.22

The exact fuzzy output values in singleton are tabulated in Table 3. The fuzzy logic output is classified as 'zero'(Z), 'small'(S), 'medium'(M), 'big'(B) or 'very big'(VB).

Table 3 Fuzzy Output for error and rate of error.

Singleton	Error (E) and Rate of Error (dE)
Z	12.5
S	22
M	31
B	41
VB	50

The FLC rules for corresponding error and rate of error are set based on 'If…then… rule' condition as tabulated according to Table 4.

Table 4 Set of fuzzy logic rules.

Error (E)/ Rate of Error (dE)	NB	NS	Z	PS	PB
NB	Z	Z	Z	S	M
NS	Z	Z	S	M	B
Z	Z	S	M	B	VB
PS	S	M	B	VB	VB
PB	M	B	VB	VB	VB

2.2.2 Adjustment to the Fuzzy Logic system

To enhance the performance of the FLC, specifically regarding rise time, overshoot, settling time, and steady-state error across various reference angles, the fuzzy rules and the boundaries for each input and output membership function can be fine-tuned through trial and error. Methods such as particle swarm optimization (PSO), genetic algorithms, or gradient descent can be incorporated into the design phase for more effective tuning. In the trial-and-error process, adjustments to the membership functions and output boundary values aim to achieve improved performance results. If performance remains unsatisfactory, further improvements to the closed-loop controller can be pursued by refining the settings for the error, rate of error, output, and rules. These iterative adjustments are critical for optimizing controller effectiveness.

2.2.3 Optimized Error and Rate of Error membership functions of the Fuzzy Logic system

Adjustments to the error membership function in fuzzy logic as illustrated in Table 5. In Table 5, the size of membership functions is reduced, facilitating a linear output across all levels as the Fuzzy membership function transitions smoothly. This configuration enhances the system's responsiveness and consistency. Adjustments to the rate of error membership function in Fuzzy Logic can be made, as shown in Table 5. These adjustments contribute to improved controller performance by refining the responsiveness of the Fuzzy Logic system. This variation allows for finer control and responsiveness in the Fuzzy Logic system.

Table 5 Optimized Membership Function (MF) of Error (E) and Rate of Error (dE). The input MFs are Negative Medium (NM), Negative Small (NS), Zero (Z), Positive Small (S) and Positive Big (PB).

MF	Error (E)	Rate of Error (dE)
NM	-3000, -1.0, -0.5	-3000, -0.45, -0.22
NS	-1.0, -0.5, 0	-0.22, -0.11, 0
Z	-0.5, 0, 1.25	0
PS	0, 1.25, 2.5	0, 0.011, 0.022
PB	1.25, 2.5, 3000	0.022, 0.045, 3000

2.2.4 Optimized Fuzzy output of Fuzzy logic system

Adjustments to the fuzzy logic output can further enhance controller performance. Table 6 leads to an output range smaller than that in Table 3. The minimum value starts at 0. This adjustment results in a broader output range compared to those tables, enhancing the flexibility and responsiveness of the controller. These modifications facilitate more precise control within the specified output regions.

Table 6 Optimized fuzzy output for error and rate of error.

Singleton	Error (E) and Rate of Error (dE)
Z	0
S	12.5
M	25
B	37.25
VB	50

2.2.5 Adjustment for Fuzzy Rules of Fuzzy Logic system

Modifying the fuzzy logic rules significantly enhances controller performance. Additionally, alternative sets of fuzzy logic rules that demonstrate a reduction in the number of rules are presented in Table 7. These adjustments facilitate improved system response and stability.

Table 7 Optimized set of rules.

Error (E)/ Rate of Error (dE)	NB	NS	Z	S	B
NB	Z	S	M	B	VB
NS	-	S	M	B	-
Z	-	S	M	B	-
S	-	S	M	B	-
B	-	S	M	B	-

2.3 Fuzzy Logic Controller with Feedforward

The FLC exhibits limitations in control bandwidth [12]. In the context of rehabilitation exercises for knee extension, the feedback controller (FC) is evaluated at various reference points to assess its control bandwidth. If the FC performs adequately at some reference angles but struggles at others, the feedforward control method, as shown in Figure 8, can address the problematic angle.

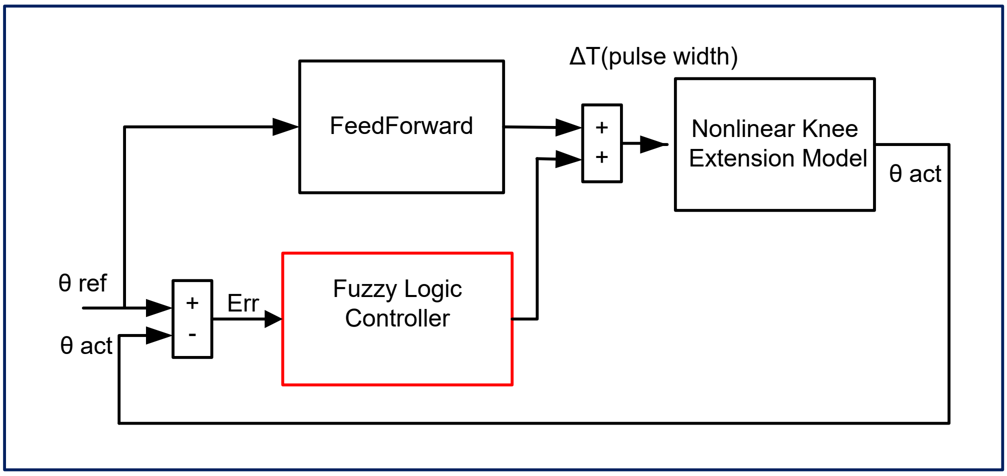

Figure 8 FLC with Feedforward assistance.

Feedforward control operates as an open-loop scheme, compensating for system dynamics without requiring information about the system states or tracking errors. Therefore, it necessitates precise knowledge of the system dynamics, including constant steady-state error, to determine appropriate gain or added values. In this study, the feedforward mechanism is connected to the input reference but may also be linked to the system output or controller output. Once the necessary value is established using the controller's rules, it is added when appropriate to enhance performance.

2.4 Fuzzy Logic Controller with Feedback Offset, Proportional and Fuzzy Integral (FI)

To address the non-linearities that lead to instability in the controlled system, particularly those caused by time delay effects, a combination of feedback offset, proportional, and Fuzzy Integral (FI) controllers is employed, as discussed in [12, 18] and shown in the block diagram as in Figure 9. In this approach, feedforward is not utilized. The feedback offset control operates as an open-loop scheme, compensating for system dynamics without requiring state information such as tracking errors.

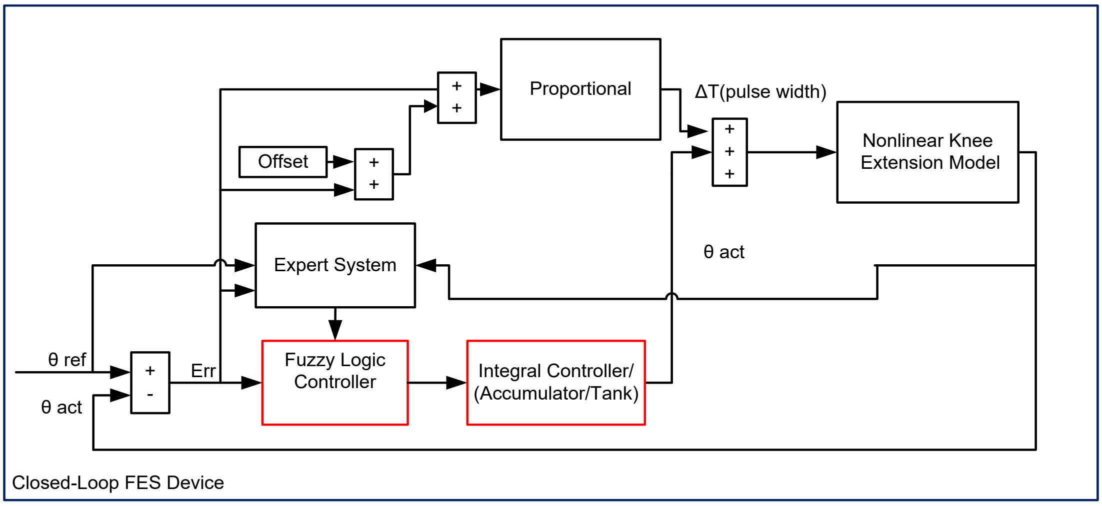

Figure 9 FLC with offset, proportional, integral and expert system.

In this configuration, the summing points for the Proportional and Integral controllers are separated, although their outputs are combined. The proportional gain is set according to the error. As it nearly approaches the target, the error value multiplying the Proportional gain must be close to the equivalent value as in Table 8. The Integral controller consists of the FLC with negative and positive outputs linked to an accumulator tank, allowing it to function as an Integral controller. Implementing this requires accurate knowledge of the system dynamics, including the reference angle and constant steady-state error. The Integral controller is designed to activate only when the steady-state error approaches zero, as predetermined, to mitigate overshoot and prevent subsequent oscillations. The reference angle and steady-state error are utilized to calculate the expected output of the FLC by correlating it with the required force or muscle torque necessary to elevate the knee to a specific angle. Understanding body mechanics is essential for determining the force or torque needed for this elevation [12, 18]. Consequently, a table linking the elevation angle, muscle torque, and expected controller pulse width output has been established, as presented in Table 8 for proportional controller.

Table 8 Reference angle, torque and pulse width for proportional controller.

Ref. Angle	**20°**	**30°**	**40°**	**50°**	**60°**	**70°**	**80°**	**90°**
Torque	2.89	4.33	5.77	7	8.67	10.11	11.5	13
Equivalent pulse width	56.67	85	113.33	127.5	170	198.33	226.67	255

The output is matched to the final FLC output. For example, at a reference point of 76°, the required torque is 11 Nm, which corresponds to a controller's pulse width output value of 213, prorated from a range of 0 to 255. This value represents the maximum expected output for the Proportional controller. To maintain this output, a small feedback offset is introduced before connecting to the summing point. This feedback offset combines with the Proportional controller gain to produce a single output value, facilitating rapid system response without overshooting while leaving some error to be addressed by the Fuzzy Integral (Fuzzy I) controller. The Proportional controller thus outputs a constant value, allowing the Fuzzy I region to operate freely. The Fuzzy I controller is designed to function more slowly to prevent unwanted overshoot that could lead to further oscillation in the system, while effectively eliminating steady-state errors.

2.5 Simulation Model Development

This section discusses the simulation model of the system and the FLC. The top-level MATLAB/Simulink model for the knee extension and feedback controller is referenced in [12, 18]. Figure 10 illustrates the internal block of the FLC feedback controller used to manage the knee extension system.

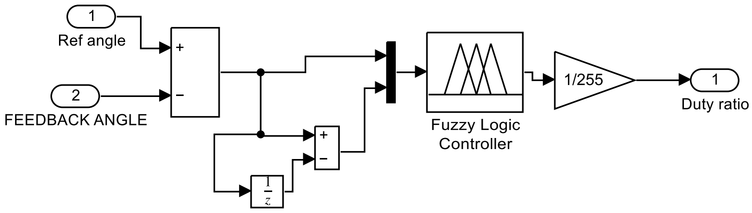

Figure 10 MATLAB/Simulink simulation model with fuzzy logic in closed-loop feedback control.

The internal block design of the knee extension model controlled by the fuzzy feedback controller (FFC) is shown in Figure 11, following the approaches outlined in [12, 18]. This figure presents the integration of the FFC with the non-linearities, illustrating the top level of the closed-loop FES system. It comprises the designed FFC alongside the knee extension model developed using MATLAB Simulink.

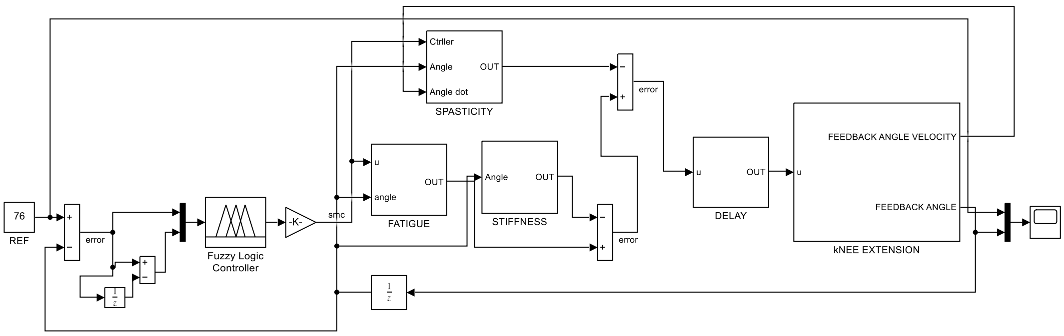

Figure 11 Knee extension model with nonlinearities in MATLAB/Simulink.

2.5.1 Feedforward Fuzzy Controller

Figure 12 illustrates the simulation model of the FFC employing feedforward (FFWD) control. In this configuration, the FFWD controller operates as an open-loop scheme connected to the reference input. Its output is added to the FFC output, effectively eliminating steady-state error and enhancing the closed-loop control bandwidth of the FFC [13].

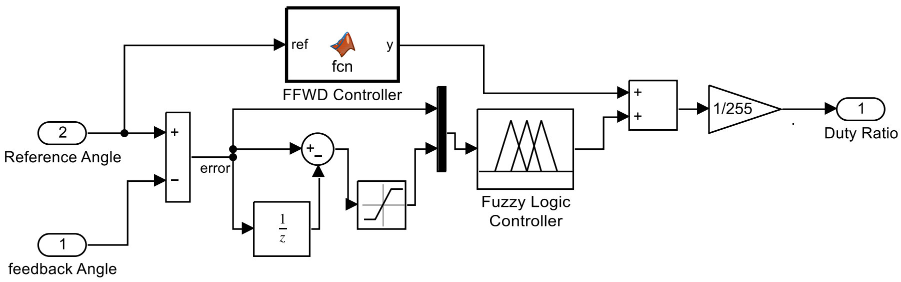

Figure 12 FFWD and FLC controllers in MATLAB/Simulink.

2.5.2 Feedback Offset, Proportional and Fuzzy Integral

As shown in Figure 13, the offset, proportional, and fuzzy integral controllers are interconnected to achieve steady and consistent output when addressing time delay non-linearity, which often causes the conventional FLC to oscillate and become uncontrollable [13]. Integrating these control elements within a closed-loop system, the complete simulation circuit aims to mitigate oscillations and eliminate steady-state errors. This is accomplished by combining the offset function, fuzzy logic, and an accumulator. Functioning as an integrator controller, the accumulator effectively integrates the fuzzy controller's output, which is calibrated to a low setting based on system performance. The fuzzy output and the accumulator tank range is pre-set to define maximum and minimum values.

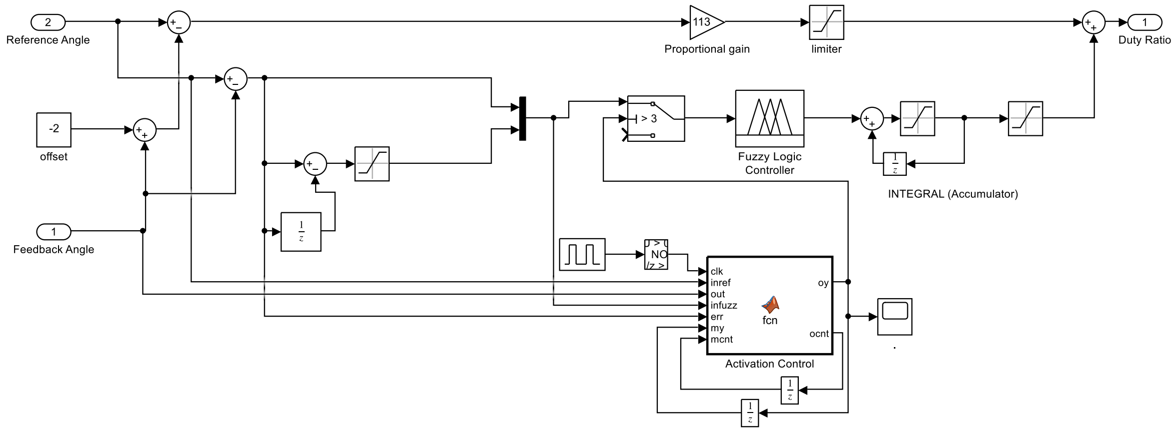

Figure 13 Simulation model of FLC with offset, and accumulator tank.

3 RESULTS AND DISCUSSION

This section presents a detailed analysis of the simulation results from the FLC . The analysis is divided into the tuning and development phase and the final testing and comparison phase. During the tuning phase, iterative adjustments were made to optimize the controller's performance, focusing on the error membership function, rate of error membership function, FLC output, and FLC rules. In the final phase, the tuned FL controller was tested under various conditions, including with and without non-linearities. A comparative analysis was also performed, contrasting the conventional FLC with the improved version (incorporating Feedforward, Feedback Offset, and Proportional Integral), showcasing their performance under these scenarios.

3.1 FLC during Tuning and Development

Figure 14 (a-d) presents the continuous knee trajectory results during the FLC tuning process for the knee extension model in closed-loop control. Figure 14(a) depicts the best result after modifying the fuzzy logic error membership function, as summarized in Table 5. This result shows a slow time response, steady-state errors at 20°, 30°, and 76°, and overshoots at 20° and 30°. Figure 14(b) presents the outcome of adjusting the rate of error membership function Table 5, showing a faster response than Figure 14(a), but still with steady-state errors and overshoots at the same reference points. Figure 14(c), based on Table 6, illustrates the best result after adjusting the output values, achieving a faster response with reduced steady-state errors and smaller overshoots at 20° and 30°. Finally, Figure 14(d), using the rules from Table 7, shows the best overall performance, with a faster response, minimal steady-state errors at all reference points, and small overshoots at 20° and 30°, indicating that modifying the fuzzy rules optimizes both speed and accuracy of the system response.

3.2 FLC during the Testing and Comparison Phase

Figure 15(a) indicates that the FLC experiences control bandwidth limitations, restricting its effectiveness across the reference signal range [12]. To resolve the control bandwidth limitations in the FLC, a feedforward controller was introduced to correct the steady-state error, particularly at the reference angle of 76°. Figure 15(b) illustrates the integration of the feedforward into the FLC, with performance results further summarized in Table 9, indicating a reduction in steady-state error. The feedforward offset significantly improves the steady-state error at the 76° reference angle. Additionally, analysis of the output responses shows minimal overshoot, highlighting the crucial role of fuzzy output offset in enhancing overall system performance.

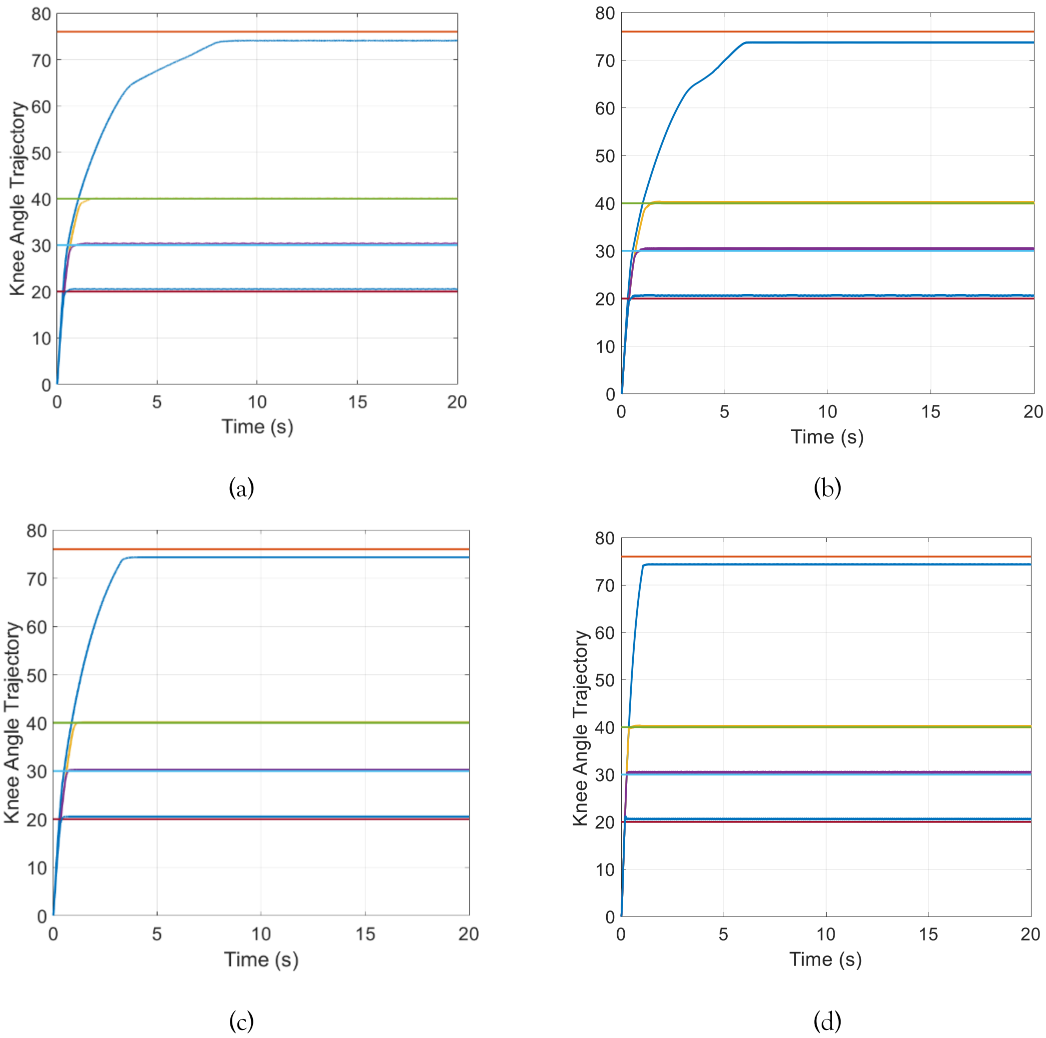

Figure 14 Knee angle response during tuning (a) Knee angle response change of error (b) change of rate of error (c) change of output (d) change of rules.

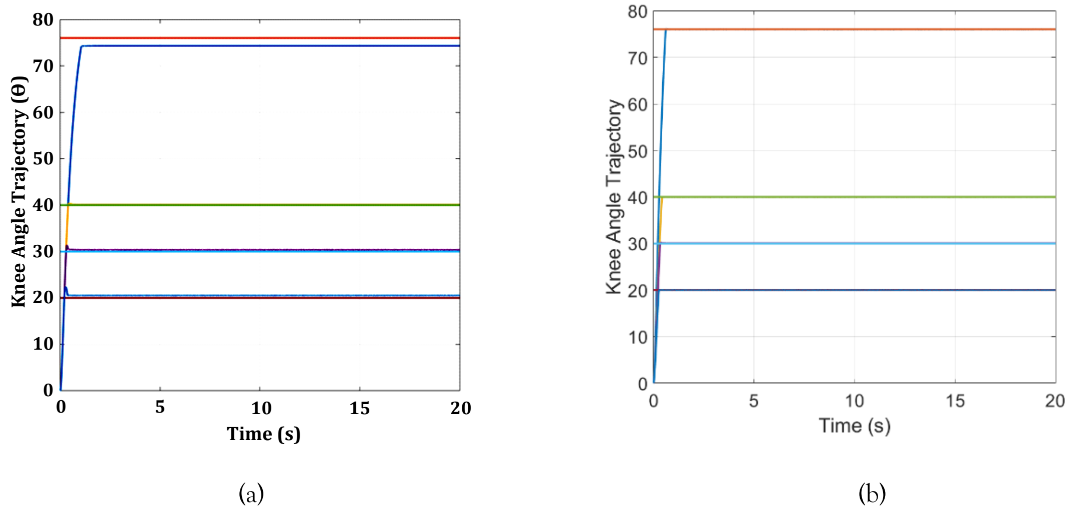

Figure 15 Knee angle response without nonlinearity (a) Knee angle response; (b) Knee angle response using FFWD. The reference angle (ref) and knee response (resp) are represented in different coloured lines as follows: (i) ref 76°: orange and resp: blue; (ii) ref 40°: light green and resp: yellow; (iii) ref 30°: light blue and resp: purple; (iv) ref 20°: red and resp: blue.

Table 9 Performance comparison of conventional FLC and FFWD FLC without nonlinearities.

Non-linearity	No nonlinearities FLC				No nonlinearities FFWD FLC			
Ref. Angle	**20°**	**30°**	**40°**	**76°**	**20°**	**30°**	**40°**	**76°**
Rise Time (s)	0.14	0.2	0.28	0.77	0.18	0.24	0.31	0.77
Settling Time (s)	0.21	0.3	0.4	1.2	0.28	0.34	0.43	1.68
Overshoot	0.527	0.403	0.096	0	0.01	0.06	0	0
Steady-state error	0.518	0.400	0.096	1.688	0	0	0	0

3.3 Closed-Loop FLC with Fatigue Nonlinearity

Under fatigue nonlinearity, the FLC without feedforward (FFWD) shows a decline in knee angle trajectory, especially at the higher reference point 76° as shown in Figure 16. This is further compounded by a control bandwidth issue, resulting in a 4° steady-state error at this critical point. To address this, feedforward was introduced, specifically targeting the 76° reference to correct the steady-state error and enhance performance before fatigue onset. As summarized in Table 10, the closed-loop controller with feedforward significantly reduced the steady-state error, improving performance at the 76° reference before fatigue sets in.

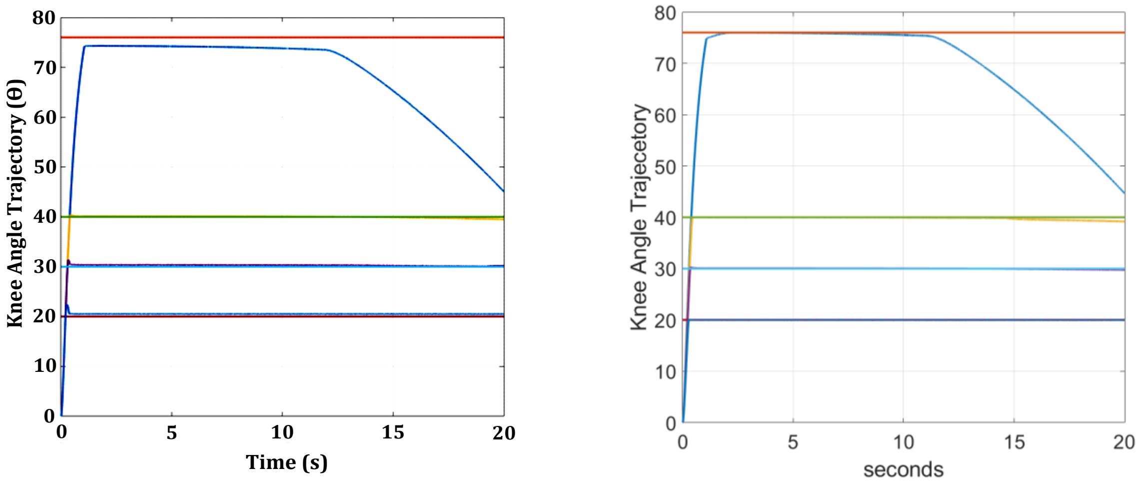

(a) (b)

Figure 16 Knee angle response with fatigue nonlinearity (a) Conventional FLC knee angle response with fatigue non-linearity (b) FFWD FLC knee angle response with fatigue. The reference angle (ref) and knee response (resp) are represented in different coloured lines as follows: (i) ref 76°: orange and resp: blue; (ii) ref 40°: light green and resp: yellow; (iii) ref 30°: light blue and resp: purple; (iv) ref 20°: red and resp: blue

Table 10 Performance comparison of conventional FLC with FFWD FLC with fatigue non-linearity.

Non-linearity	Fatigue FLC				Fatigue FFWD FLC			
Ref. Angle	**20°**	**30°**	**40°**	**76°**	**20°**	**30°**	**40°**	**76°**
Rise Time (s)	0.14	0.2	0.28	0.77	0.18	0.24	0.31	0.77
Settling Time (s)	0.21	0.3	0.4	-	0.28	0.34	0.43	1.68
Overshoot	0.5314	0.3959	0.09205	-1.711	0.01	0.06	0	0
Steady-state error	-0.5175	-0.3996	-0.09392	1.711	0	0	0	0

3.4 Closed-Loop FLC with stiffness nonlinearity

When tested with stiffness nonlinearity, the conventional FLC without feedforward (FFWD) exhibited a 4° steady-state error in the knee angle trajectory at the high reference point of 76°. This issue is attributed to a control bandwidth limitation, resulting in the same 4° error. The incorporation of feedforward (FFWD) into the system corrected the steady-state error, particularly at the 76° reference point, significantly improving the overall system performance. The closed-loop controller's performance is summarized in Table 11, highlighting the reduction in steady-state errors at the 76° reference point.

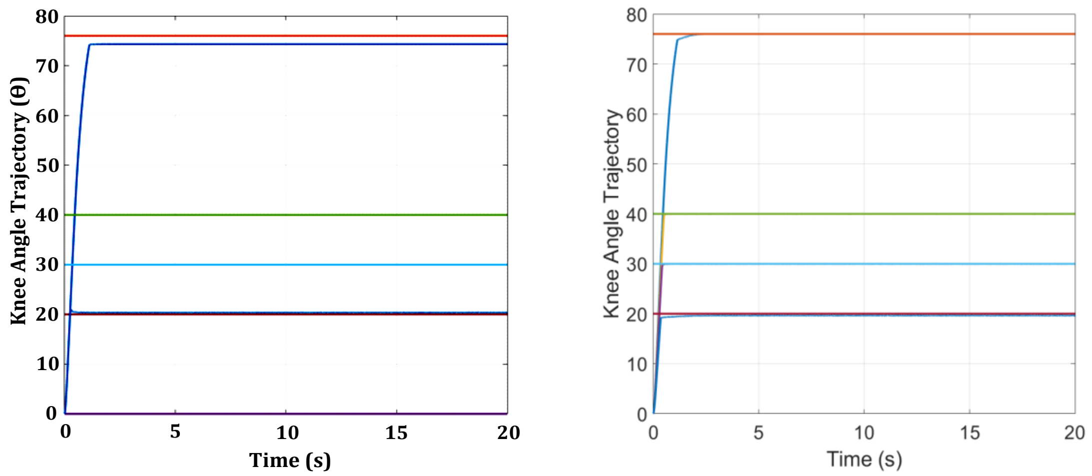

(a) (b)

Figure 17 Knee angle response with stiffness nonlinearity (a) Conventional FLC knee angle response with stiffness nonlinearity (b) FFWD FLC knee angle response with stiffness. The reference angle (ref) and knee response (resp0 are represented in different coloured lines as follows: (i) ref 76°: orange and resp: blue; (ii) ref 40°: light green and resp: yellow; (iii) ref 30°: light blue and resp: purple; (iv) ref 20°: red and resp: blue

Table 11 Performance comparison between conventional FLC and FFWD FLC with stiffness non-linearity.

Gain Settings	Stiffness FLC				Stiffness FFWD FLC			
Ref. Angle	20°	30°	40°	76°	20°	30°	40°	76°
Rise Time (s)	0.17	0.25	0.34	0.82	0.18	0.24	0.3	0.41
Settling Time (s)	0.26	0.36	0.47	-	0.27	0.33	0.41	0.58
Overshoot	0.385	0.2461	0.0963	-	0.14	0.18	0.09	0.13
Steady-state error	-0.3651	-0.2332	-0.0963	1.688	0.091	0.0437	0.1047	0.10

3.5 Closed-Loop FLC with spasticity nonlinearity

When tested under spasticity nonlinearity, the FLC without feedforward (FFWD) exhibited a 4° steady-state error in the knee angle trajectory, particularly at the 76° reference point. This error is linked to control bandwidth limitations. The introduction of feedforward aims to correct this error, especially at 76°, improving overall performance. As shown in Table 12, integrating feedforward into the FLC significantly reduced the steady-state error, particularly under spasticity nonlinearity conditions.

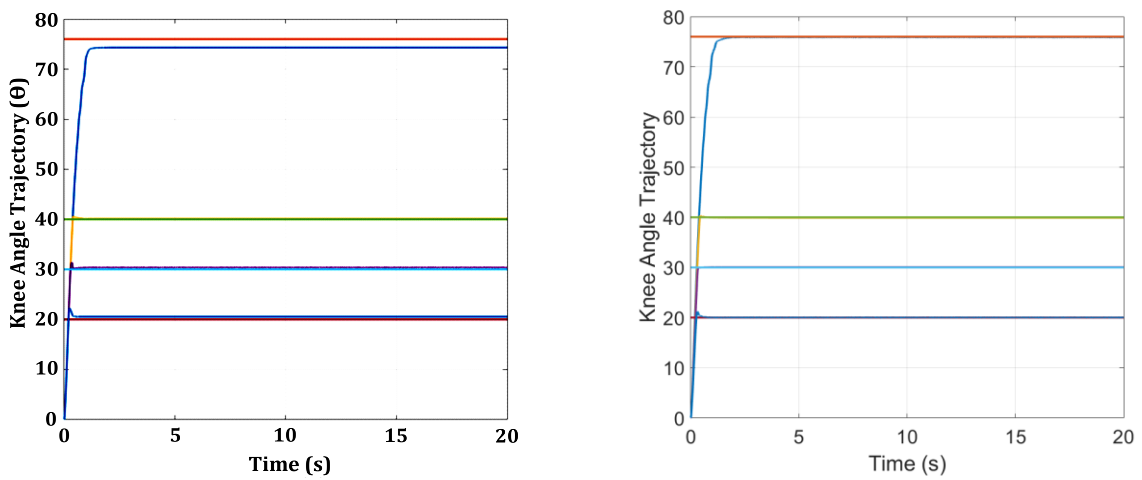

(a) (b)

Figure 18 Knee angle response with spasticity nonlinearity (a) Conventional FLC knee angle response with spasticity nonlineraity (b) FFWD FLC knee angle response with spasticity. The reference angle (ref) and knee response (resp) are represented in different coloured lines as follows: (i) ref 76°: orange and resp: blue; (ii) ref 40°: light green and resp: yellow; (iii) ref 30°: light blue and resp: purple; (iv) ref 20°: red and resp: blue

Table 12 Performance comparison between conventional FLC and FFWD FLC with spasticity non-linearity.

Gain Settings	Spasticity FLC				Spasticity FFWD FLC			
Ref. Angle	**20°**	**30°**	**40°**	**76°**	**20°**	**30°**	**40°**	**76°**
Rise Time (s)	0.14	0.21	0.29	0.81	0.19	0.24	0.3	0.81
Settling Time (s)	0.21	0.29	0.39	-	0.27	0.34	0.42	1.16
Overshoot	0.5171	0.3944	0.0965	-1.711	0	0.006	0	0
Steady-state error	-0.4875	-0.3296	-0.0919	1.711	0	-0.0059	0.076	0.1507

3.6 Closed-Loop FLC with time delay nonlinearity

The conventional FLC struggles with controlling systems that experience time delays, often resulting in instability and oscillations [12]. To mitigate the instability and oscillation issues, a modified approach incorporating feedback offset, proportional control, and a fuzzy integrator with an accumulator tank was introduced to improve controller response. As summarized in Table 13, this approach reduced both steady-state errors and oscillations, achieving a minor steady-state error of 0.5°. Although system response time increased due to the accumulator's influence, stability was eventually restored as oscillations diminished, improving overall performance.

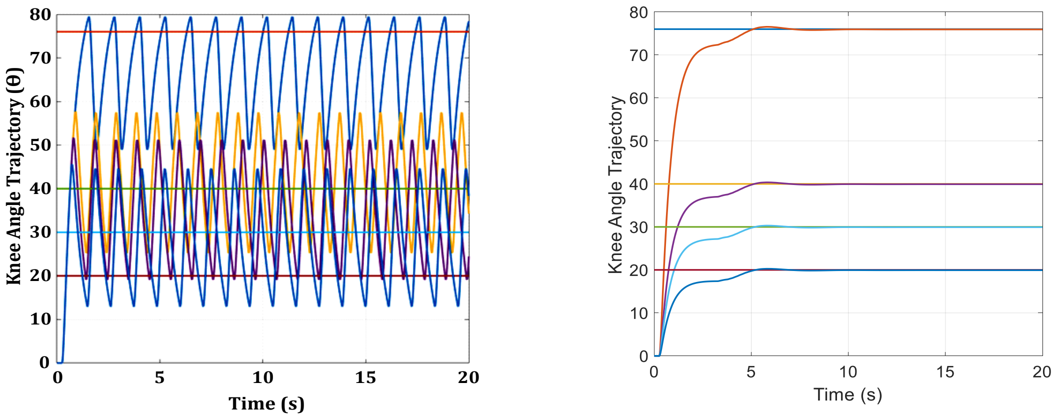

(a) (b)

Figure 19 Knee angle response with time delay nonlinearity (a) Conventional FLC knee angle response with time delay nonlinearity (b) Feedback Offset, Proportional and Fuzzy Integral FLC knee angle response with time delay nonlinearity. The reference angle (ref) and knee response (resp) are represented in different coloured lines as follows: (i) ref 76°: orange and resp: blue; (ii) ref 40°: light green and resp: yellow; (iii) ref 30°: light blue and resp: purple; (iv) ref 20°: red and resp: blue

Table 13 Performance of FLC controller with time delay.

Gain Settings	Time Delay (250 ms)				Time Delay (250 ms) Feedback offset, Proportional control, and Fuzzy Integrator			
Ref. Angle	**20°**	**30°**	**40°**	**76°**	**20°**	**30°**	**40°**	**76°**
Rise Time (s)	0.14	0.2	0.28	0.77	3.56	2.27	1.77	1.47
Settling Time (s)	-	-	-	-	4.9	4.77	4.66	4.42
Overshoot	-	-	-	-	2.948	3.107	3.28	3.794
Steady-state error	-	-	-	-	1.502	1.532	1.63	1.92

3.7 Comparison of Closed-Loop Conventional FLC Performance with Other Controllers

To evaluate the performance of the fine-tuned conventional FLC without any associated assistance of FFWD, Offset, Proportional, Integral, etc., to other established control methods by focusing on key metrics such as rise time, settling time, overshoot, and steady-state error as shown in Table 14. The comparative analysis aims to highlight FLC's advantages and limitations, contributing to the development of more effective control strategies in engineering applications.

The proposed conventional FLC demonstrates superior performance across all key control metrics compared to other methods. In terms of rise time, FLC achieves a value of 0.28 seconds, placing it among the faster methods. Although Neto, et al. [22] (ZN-PID) is 28.6% faster in rise time, this has significant trade-offs in other areas, particularly in settling time and overshooting. The proposed conventional FLC outperforms Neto, et al. [22] (ZN-PID) in settling time, achieving stabilization 96.3% faster. This indicates that while FLC may be slightly slower to initiate, it reaches system stability much more quickly and fficiently.

In terms of overshoot, the proposed conventional FLC excels with only 0.096°, a vast improvement over methods like Neto, et al. [22] (ZN-PID), which shows 99.8% higher overshoot. This makes FLC particularly effective in maintaining system stability and avoiding excessive oscillations, which can lead to damage or instability in control systems. The proposed conventional FLC maintains minimal error at 0.096° for steady-state errors, proving its long-term accuracy. Compared to traditional PID methods such as Benahmed's trial-and-error PID, which has an error of 99% higher compared to our proposed conventional FLC. Therefore, our proposed conventional FLC can be considered as the second most precise and reliable feedback control method after the SMC feedback control method from our previous work [12].

Table 14 Comparison of conventional FLC performance with other research work.

Proposed by:	Type of Controller	Ref Angle (Deg)	Rise Time (s)	Settling Time (s)	Overshoot (Deg)	Steady State Error (Deg)
Neto, et al. [22]	ZN- PID	40°	0.20	10.99	50.8°	0.9°
Neto, et al. [22]	PWA-PID	40°	0.32	9.5	14.4°	0.3°
Lynch and Popovic [5]	PID (Trial and error)	40°	2.24	5.0	0°	11.07°
Benahmed, et al. [10]	PID (Trial and error)	40°	2.20	7.69	5.72°	16.31°
S.Arof, et al. [18]	PID (Pole placement)	40°	2.22	3.75	0°	0.65°
Lynch and Popovic [5]	Sliding Mode	40°	0.46	1.19	12.6°	7.4°
S.Arof, et al. [12]	Sliding Mode	40°	0.31	0.44	0.0068°	0.0054°
This work	FLC	40°	0.28	0.4	0.096°	0.096°

The proposed conventional FLC also shows superior control over critical nonlinearities and time delays. Unlike traditional methods, which often struggle with excessive overshoots and long settling times, FLC's performance is highly efficient. It ensures that the control system reaches stability quickly and with minimal oscillations or deviations. Even compared to Sliding Mode Controllers, which offer high stability, FLC is up to 9.6% faster in rise time and 9.09% faster in settling time while maintaining similar stability levels.

In summary, the proposed conventional FLC achieves the best overall performance excelling in both rise and settling time, overshoot, and error. It outperforms traditional PID methods in most metrics and achieves near-perfect control for this application. In terms of stability, the sliding mode controllers from Arof, et al. [18] offers the smallest steady-state error but are slightly slower in settling time compared to FLC.

4 CONCLUSION

This study focuses on optimizing FLC tuning to enhance system performance by modifying error membership functions, rate of error membership functions, fuzzy outputs, and fuzzy rules. Notable performance gains are achieved with feedforward control, especially in eliminating steady-state error at 76˚. Additional improvements are observed in mitigating time delays by incorporating feedback offset and a proportional fuzzy integrator. All controller configurations can be stored in memory or a look-up table, allowing the design of adaptive control laws. Although overshoot persists, further optimization of input membership functions for error and rate of error using methods like PSO, genetic algorithms, or gradient descent can improve performance. These findings provide important inputs for future research work aiming adaptive closed-loop FLC feedback controller for nonlinear systems.

ACKNOWLEDGEMENT

The authors would like to thank the Ministry of Higher Education (MOHE) Malaysia and the Universiti Teknologi MARA, Cawangan Pulau Pinang, for the research facilities provided during the experimental work. The APC and research work were funded by the Ministry of Higher Education (MOHE) Malaysia through the Fundamental Research Grant Scheme (FRGS) with grant number FRGS/1/2021/TK0/UITM/03/1.

REFERENCES

[1] J. J. A. a. J. C. Gillette, "Using electrical stimulation to control standing posture," *IEEE Control Systems Magazine,* 2001.

[2] T. A. Thrasher, H. M. Flett, and M. R. Popovic, "Gait training regimen for incomplete spinal cord injury using functional electrical stimulation," *Spinal Cord,* vol. 44, no. 6, pp. 357-61, Jun 2006, doi: 10.1038/sj.sc.3101864.

[3] Y. Tu, Matthews, Glenn I.Lee, Shuenn-yuh,Fang, Qiang, "A closed loop microstimulator controlled by muscle fatigue status and function impairment level for upper limb rehbilitation," presented at the International Symposium on Bioelectronics and Bioinformatics (ISBB), , Beijing, China, 2015, 2015.

[4] T. B. A. Kralj, and R. Turk, , "Enhancement of Gait Restoration in Spinal Injured Patients by Functional Electrical Stimulation," *Clinical Orthopedic and Related Research.,* vol. vol. 233,, pp. pp. 34–43, , 1988, doi: 10.1097/00003086-198808000-00006.

[5] C. L. Lynch and M. R. Popovic, "A comparison of closed-loop control algorithms for regulating electrically stimulated knee movements in individuals with spinal cord injury," *IEEE Transactions on Neural Systems and Rehabilitation Engineering,* vol. 20, no. 4, pp. 539-548, 2012, doi: 10.1109/TNSRE.2012.2185065.

[6] E. N. Saharul Arof, Saiful Zaimy Yahaya, Nor Haslina Ibrahim, and Hamzah Arof, "Features Extraction from a Second-Order Black Box Model Matched to the Veltink Model for a System Identification of Knee Extension for Control Law and Formulations of Close-Loop Controller rehabilitation Using Functional Electrical Stimulatio," in *Progress in Engineering Technology IV*, vol. 169: Springer, 2022, pp. 62-78.

[7] N. M. N. Saharul Arof, Emilia Noorsal, Saiful Zaimy, and a. H. A. Zakaria Hussein, "Formulations After Features Extraction of Veltink to Second-Order Critical Damped Black Box Model for Observer Formation Representing Knee Extensio," in *Progress in Engineering Technology IV*: Springer, 2022, pp. 168-178.

[8] F. Previdi and E. Carpanzano, "Design of a gain scheduling controller for knee-joint angle control by using functional electrical stimulation," *IEEE Transactions on Control Systems Technology,* vol. 11, no. 3, pp. 310-324, 2003, doi: 10.1109/TCST.2003.810380.

[9] S. Jezernik, R. G. Wassink, and T. Keller, "Sliding mode closed-loop control of FES: controlling the shank movement," *IEEE Trans Biomed Eng,* vol. 51, no. 2, pp. 263-72, Feb 2004, doi: 10.1109/TBME.2003.820393.

[10] S. Benahmed, M. Tadjine, and O. Kermia, "Adaptive super twisting controller: In search of a universal controller for the paraplegic knee movement using FES," *2017 5th International Conference on Electrical Engineering - Boumerdes, ICEE-B 2017,* vol. 2017-Janua, pp. 1-6, 2017, doi: 10.1109/ICEE-B.2017.8192013.

[11] H. Kawai, M. J. Bellman, R. J. Downey, and W. E. Dixon, "Closed-Loop Position and Cadence Tracking Control for FES-Cycling Exploiting Pedal Force Direction With Antagonistic Biarticular Muscles," pp. 1-13, 2017.

[12] S. Arof *et al.*, "Adaptive Sliding Mode Feedback Control Algorithm for a Nonlinear Knee Extension Model," *Machines,* vol. 11, no. 7, 2023, doi: 10.3390/machines11070732.

[13] S. C. A. a. M. O. Tokhi, "Comparative assessment of two fuzzy logic based control approaches for a flywheel and electrical clutch assist mechanism in FES cycling," presented at the 19th International Conference on Methods and Models in Automation and Robotics (MMAR), , Miedzyzdroje, Poland, , 2014.

[14] M. A. Alouane, H. Rifai, Y. Amirat, and S. Mohammed, "Cooperative Control for Knee Joint Flexion-Extension Movement Restoration," pp. 5175-5180, 2018.

[15] C. N. T. Sahil Shah, Omer T. Inan and Jennifer Hasler, "A Proof-of-Concept Classifier for Acoustic Signals from the Knee Joint on a FPAA," 2016, doi: 10.1109/ICSENS.2016.7808748.

[16] Cheryl.L.Lynch, D. Sayenko, and M. R. Popovic, "co contraction of antagonist muscles during knee exension against gravityu:insight for cuntional electricl stimulation control design," ed, 2012.

[17] S. Sakaino, T. Kitamura, N. Mizukami, and T. Tsuji, "High-precision control for functional electrical stimulation utilizing a high-resolution encoder," *IEEJ Journal of Industry Applications,* Article vol. 10, no. 2, pp. 124-133, 2021, doi: 10.1541/ieejjia.20004260.

[18] S. Arof *et al.*, "Pole placement tuning of proportional integral derivative feedback controller for knee extension model," *Indonesian Journal of Electrical Engineering and Computer Science,* vol. 34, no. 3, 2024, doi: 10.11591/ijeecs.v34.i3.pp1566-1581.

[19] E. Noorsal, S. Arof, S. Z. Yahaya, Z. Hussain, D. Kho, and Y. Mohd Ali, "Design of an FPGA-Based Fuzzy Feedback Controller for Closed-Loop FES in Knee Joint Model," *Micromachines,* vol. 12, no. 8, p. 968, 2021.

[20] A. A. Rizky Mayardiyah Syafitri Pandiangan, Andra Risciawan,Siti Halimah Baki,Rudy Dikairono, "Design of Fuzzy Logic Control in Functional Electrical Stimulation (FES) Cycling Exercise for Stroke Patients," presented at the 2020 International Conference on Computer Engineering, Network, and Intelligent Multimedia (CENIM), Surabaya, Indonesia,, 2020.

[21] M. K. I. Ahmad, A. U. Shamsudin, Z. A. Soomro, R. Abdul Rahim, B. S. K. S. M. Kader Ibrahim, and M. S. Huq, "Closed-loop Functional Electrical Stimulation (FES) – cycling rehabilitation with phase control Fuzzy Logic for fatigue reduction control strategies for stroke patients," *Sinergi,* vol. 28, no. 1, 2023, doi: 10.22441/sinergi.2024.1.007.

[22] D. L. A. Neto, A. F. O. A. Dantas, T. F. de Almeida, J. A. de Lima, and E. Morya, "Comparison of Controller's Performance for a Knee Joint model based on Functional Electrical Stimulation Input," presented at the 2021 10th International IEEE/EMBS Conference on Neural Engineering (NER), 2021.